Available online at www.sciencedirect.com
SCIENCE DIRECT®
Coordination Chemistry Reviews 245 (2003) 85–93
COORDINATION CHEMISTRY REVIEWS
www.elsevier.com/locate/ccr

# Catalytic activation of dioxygen by oximatocobalt(II) and oximatoiron(II) complexes for catecholase-mimetic oxidations of *o*-substituted phenols

László I. Simándi*, Tatiana M. Simándi, Zoltán May, Gábor Besenyei

*Chemical Research Center, Institute of Chemistry, Hungarian Academy of Sciences, P.O. Box 17, Budapest 1525, Hungary*

Received 18 October 2002; accepted 14 March 2003

## Contents



## Abstract

Bis(dimethylglyoximato)cobalt(II) and -iron(II) complexes, referred to as cobaloxime(II) and ferroxime(II), respectively, containing rigid equatorial macrocycles stabilized by hydrogen bonding, are functional catecholase and phenoxazinone synthase models, but show no catechol dioxygenase type activity. We have studied the oxidation of 3,5-di-*tert*-butylcatechol ($DBCatH_2$) and 2-aminophenol (AP) as model substrates with the objective of elucidating the mechanisms of these reactions, using a combination of techniques including identification of free-radical intermediates by ESR spectroscopy and UV–vis spectrophotometry of semiquinone anion radical adducts of cobaloxime and ferroxime species. Detailed kinetic studies of the catecholase-mimetic oxidations reveal a general mechanistic pattern involving reversible formation of ternary catalyst–substrate–dioxygen complexes, which are key intermediates capable of H-atom abstraction from the substrates. The resulting semiquinone anion-radical intermediate and its adducts with the catalyst complexes have been detected by ESR spectroscopy. They contain a unidentate catecholato ligand as shown by the adduct of cobaloxime(II), which has been isolated and characterized by X-ray diffraction. Our work has led to the conclusion that the lack of catechol dioxygenase activity in the case of ferroxime(II) is due to the rigid equatorial macrocycle, which prevents bidentate catechol coordination. To further test this hypothesis, we have synthesized and studied analogous iron(II) complexes with flexible quadridentate and quinquedentate dioximato Schiff-base ligands. In line with expectations, these new complexes exhibit both catecholase and catechol dioxygenase activity.


*Keywords:* Bioinorganic chemistry; Catecholase mimics; Cobaloxime(II); Dioxygen activation; Biomimetic oxidation

## 1. Introduction

There is continuing interest in mechanistic studies on the catalytic oxidation of catechols by transition metal

* Corresponding author. Tel.: +36-1-325-7750; fax: +36-1-325-7554.
*E-mail address:* simandi@chemres.hu (L.I. Simándi).

0010-8545/$ – see front matter © 2003 Elsevier B.V. All rights reserved.
doi:10.1016/S0010-8545(03)00057-2

complexes. These reactions are functional models of dioxygenase and catecholase enzymes, which, in combination with monooxygenases, play key roles in the metabolism of aromatic compounds. Dioxygenases effect cleavage of the catechol ring with incorporation of two oxygen atoms into the products, whereas catecholases convert catechols to *o*-quinones. Functional catechol dioxygenase and catecholase models [1a,1b] based on iron [1c,1d,1e], copper [1f,1k], manganese [1i,1j] and cobalt [1g,1h] complexes have been designed and extensively studied with respect to their structure, kinetics and mechanisms. The term 'functional model' is generally applied to a low-molecular metal complex that catalyzes the same (or a closely related) reaction as does the metalloenzyme to be mimicked. In combination with 'structural models', which mimick various structural features, functional models constitute the basis for the modelling approach in the study of metalloenzymes, which regards metalloenzyme active sites as metal complexes embedded in a protein matrix. The study of 'biomimetic' reactions catalyzed by functional metalloenzyme models helps understand the mechanisms of metalloenzyme action and assists the design of metal complex catalysts for specific purposes (bioinspired catalysis).

A typical feature of the functional dioxygenase models is that they also catalyze catechol oxidation to the *o*-quinone (catecholase reaction). The reverse is not true, however, there are models which are only effective catalysts of the catecholase reaction. The difference in catalytic activity of the models is obviously due to mechanistic factors determined by structural differences. We have been interested in elucidating the reasons of the dioxygenase vs catecholase selectivity. Our strategy has been to proceed from clean catecholase models and modify their structure so that dioxygenase activity would appear. Our approach has been essentially mechanistic, which required kinetic studies in combination with a search for intermediates by various techniques. In this review, we describe research concerned with catecholase models of the cobaloxime(II) and ferroxime(II) type, but related phenoxazinone synthase and oxygenase model systems are also treated. The observed kinetic behavior shows extensive similarity between the individual catalytic systems, reflecting a common type of free-radical mechanism, involving H-atom abstraction by a superoxometal complex from a substrate OH group.

The square-planar bis(dimethylglyoximato) complexes of cobalt(II) and iron(II), referred to as cobaloxime(II) [1–3] and ferroxime(II) [4], respectively, shown in Fig. 1, activate dioxygen under ambient conditions and exhibit remarkable catalytic activities in the oxidation of substituted phenols and anilines. Axial coordination of a ligand such as py, MeIm, $Ph_3P$, $Ph_3As$, $Ph_3Sb$, etc., increases the activity, but the 2:1 complexes are unreactive.

In this review, mechanistic studies on the catalytic oxidation of *o*-substituted phenols and anilines are described with special reference to catecholase-type reactions, i.e., oxidative dehydrogenations to the corresponding *o*-quinones, *o*-quinone mono- and diimines, as well as other products derived from their further transformations.

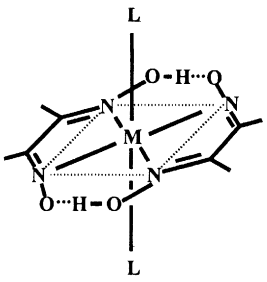


**1) Cobaloximes**
**M = Co(II)**
**L = $Ph_3P$, $Ph_3As$, $Ph_3Sb$**
**2) Ferroximes**
**M = Fe(II)**
**L = MeOH, MeIm**

Fig. 1. Structure of cobaloxime(II) and ferroxime(II) complexes.

To obtain information about the transition from catecholase to dioxygenase activity, we have synthesized ferroxime(II)-like dioximatoiron(II) complexes, which lack the rigid equatorial macrocyle imparting full catecholase selectivity. The new complexes with flexible quadridentate and quinquedentate dioximato Schiff-base ligands (Fig. 12) still exhibit catecholase activity, but in the presence of TEA intradiol cleavage products are also formed due to catechol dioxygenase activity.

## 2. Catecholase-mimetic oxidations with $O_2$ catalyzed by cobaloxime(II) derivatives

### *2.1. Reaction of cobaloxime(II) with dioxygen*

The rate constants for $O_2$ binding ($k_1$) are usually very large and kinetic studies require the stopped-flow technique, in which a solution of the cobalt complex prepared under an inert gas is rapidly mixed with an $O_2$-saturated solution. The reaction is then monitored spectrophotometrically. The problem of inert storage was eliminated in the case of $[Co(Hdmg)_2]$, cobaloxime(II), by preparing the cobalt complex in the mixing chamber from $Hdmg^-$ and cobalt perchlorate [5]. This was made possible by the fact that the formation of $[Co(Hdmg)_2]$ is much faster than its subsequent reaction with $O_2$.

### *2.2. Oxidations catalyzed by cobaloxime(II) complexes*

The catalytic activity of cobaloxime(II) derivatives $[Co(Hdmg)_2L_2]$, where $H_2dmg$ is dimethylglyoxime, and L is $Ph_3P$, py and $Et_3N$, in the oxidative dehydrogenation of hydroquinone and hydrazobenzene and in oxygen insertions into some organic substrates at room temperature and

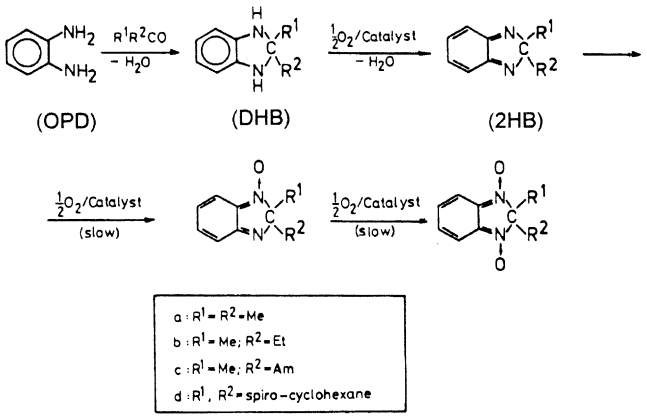


Fig. 2. Cobaloxime(II)-catalyzed oxidation of OPD in ketone solvents.

atmospheric dioxygen pressure has first been recognized in the 1980s [6–9].

$$\text{R—NC} \xrightarrow{O_2/\text{cat.}} \text{R—NCO}$$

$$\text{Ph—NO} \xrightarrow{O_2/\text{cat.}} \text{Ph—NO}_2$$

### 2.3. Oxidation of o-phenylenediamine

The cobaloxime(II) derivatives $[Co(Hdmg)_2(Ph_3P)_2]$ and $[Co(Hdmg)_2py_2]$, where $H_2dmg$ is dimethylglyoxime, are catalysts for the oxidation of *o*-phenylenediamine (OPD) by atmospheric $O_2$ at ambient temperature [10]. In acetone, methyl ethyl ketone or cyclohexanone as solvents, cyclization to 2,2-disubstituted dihydrobenzimidazoles (DHB) is followed by dehydrogenation to 2,2-disubstituted 2H-benzimidazoles (2HB) (Fig. 2). Acetaldehyde affords 2-methylbenzimidazole in a similar way. Interestingly, Co(II) salts exert a similar catalytic effect [11] (Fig. 3).

### 2.4. Oxidation of 2-aminophenol

Cobaloxime(II) derivatives $[Co(Hdmg)_2L_2]$, where $Hdmg^- =$ dimethylglyoximato(1−), and $L = PPh_3$, $AsPh_3$, $SbPh_3$, catalyze the oxidative dehydrogenation of 2-aminophenol (AP) at room temperature and 1 bar $O_2$ in MeOH [12]. The reaction product is 2-aminophenoxazine-3-one (APX) formed in quantitative yield according to the stoichiometric equation of Fig. 4.

This system can be regarded as a functional model of phenoxazinone synthase, which is involved in the biosynthesis

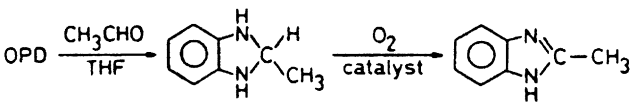


Fig. 3. Cobaloxime(II)-catalyzed oxidation of OPD in the presence of acetaldehyde.

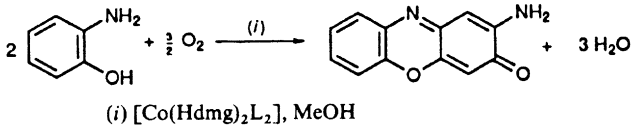


Fig. 4. Cobaloxime(II)-catalyzed oxidation of AP.

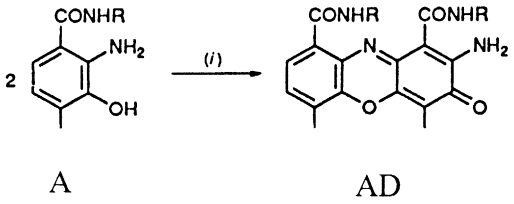


Fig. 5. The biosynthesis of AD.

of Actinomycin D (AD), a naturally occurring antineoplastic agent, from the AP derivative A (Fig. 5).

The kinetics of oxidation of AP in the presence of $[Co(Hdmg)_2(AsPh_3)_2]$ has been interpreted [13] in terms of a mechanism consisting of the steps shown in Fig. 6.

Upon dissolution of the catalyst precursor in MeOH one of the axial $Ph_3As$ ligands dissociates, generating the active pentacoordinate $[Co(Hdmg)_2(AsPh_3)]$ catalyst, denoted by $Co^{II}$. The key intermediate is the superoxocobaloxime derivative $Co^{III}(O_2)$, which abstracts an H-atom from the AP substrate via an H-bonded species X. The aminophenoxyl radical (AP•) produced is further oxidized to *o*-benzoquinone monoimine (BQMI), which is an intermediate on the path to APX formation (not shown in

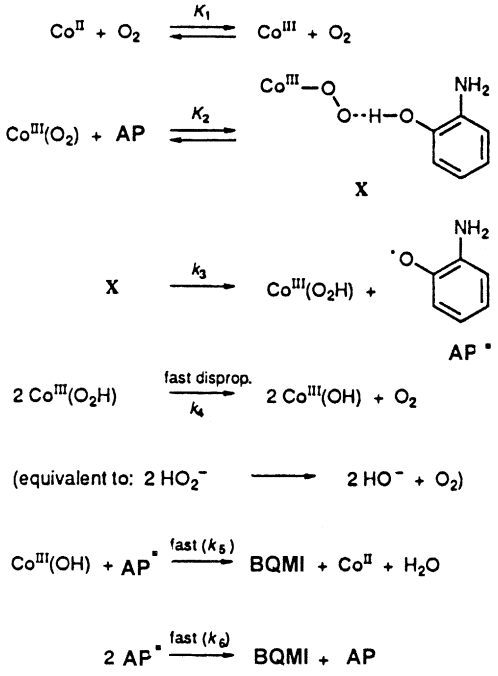


Fig. 6. Proposed mechanism of AP oxidation.

Table 1
Kinetic and equilibrium data for oxidations with $O_2$ catalyzed by cobaloxime(II) and ferroxime(II) ($T = 25\,^{\circ}C$, 1 atm, solvent MeOH)

| Catalyst | Substrate | Kinetic equilibrium [Ref.] | $k_3$ ($s^{-1}$) | $K_1K_2$ ($M^{-2}$) | $k_3K_1K_2$ ($M^{-2}\,s^{-1}$) |
|---|---|---|---|---|---|
| Cobaloxime(II) | $DBCatH_2$ | 4 [16] | $3.83 \times 10^{-2}$ | $5.06 \times 10^{4}$ | $2.00 \times 10^{3}$ |
| Cobaloxime(II)[a] | $DBCatH_2$ | 4 [15] | $6.96 \times 10^{-2}$ | $6.91 \times 10^{3}$ | $4.80 \times 10^{2}$ |
| Cobaloxime(II) | AP | 2 [13] | $1.56 \times 10^{-2}$ | $7.20 \times 10^{4}$ | $1.12 \times 10^{3}$ |
| Cobaloxime(II) | $H_2StQ$ | 21 [17] | $4.42 \times 10^{-3}$ | $1.51 \times 10^{4}$ | $6.67 \times 10$ |
| Ferroxime(II) | $DBCatH_2$ | 29 [4] | $7.30 \times 10^{-3}$ | $7.58 \times 10^{4}$ | $5.53 \times 10^{2}$ |
| $Fe(Hdmed)^+$ | $DBCatH_2$ | 35 [18] | NA | NA | $2.90 \times 10^{2}$ |
| $Fe(Hdmpd)^+$ | $DBCatH_2$ | 35 [18] | NA | NA | $6.10 \times 10$ |
| $Fe(Hdmdt)^+$ | $DBCatH_2$ | 35 [18] | NA | NA | $5.65 \times 10$ |

[a] Solvent: benzene.

Fig. 6). EPR studies provide evidence for formation of the AP• free radical as intermediate [12].

The kinetic equation corresponding to the mechanism shown in Fig. 6 can be derived assuming that $K_1$ and $K_2$ are pre-equilibria involving the catalyst, $O_2$ and the AP substrate. The rate-determining step ($k_3$) is H-atom transfer within the ternary complex X. Of significance is that only a single coordination site is available in the cobaloxime(II) catalyst $[Co(Hdmg)_2(AsPh_3)]$. Due to the $d^7$ configuration of the central cobalt(II) ion, this site is tailor-made for dioxygen, affording the superoxocobaloxime(III). The kinetic behavior requires association with the substrate too, but no coordination site is free. Therefore, it is an H-bonding interaction of the type shown in Fig. 6 that holds the ternary complex X together. Using the balance equation for the catalyst, the following general kinetic equation is obtained for a phenol-type substrate S:

$$v_{in} = k_3 \frac{K_1K_2[O_2][S]_o[Co]_o}{1 + K_1[O_2]\{1 + K_2[S]_o\}} \quad (1)$$

where $v_{in}$ is the initial rate of $O_2$ uptake ($M\,s^{-1}$).

The kinetic equation (2) valid for the oxidation of AP can be obtained by substituting AP for S, and introducing the assumption that $1 \ll K_2[AP]_o$. The result is

$$v_{in} = k_3 \frac{K_1K_2[O_2][AP]_o[Co]_o}{1 + K_1K_2[O_2][AP]_o} \quad (2)$$

Eq. (4) was used for evaluating the kinetic results and determining the parameters $k_3$ and $K_1K_2$ [13], which are listed in Table 1.

### 2.5. Oxidation of 3,5-di-tert-butylcatechol

The oxidation of 3,5-di-*tert*-butylcatechol ($DBCatH_2$) by $O_2$ to the corresponding 1,2-benzoquinone (DTBQ) is catalyzed by the cobaloxime $[Co(Hdmg)_2(PPh_3)_2]$ in methanol [14] and benzene [15]. The overall stoichiometry is given by the equation:

$$DBCatH_2 + 0.5O_2 \rightarrow DTBQ + H_2O \quad (3)$$

An intermediate catecholatocobaloxime (III) has been isolated from the reacting mixture. Its molecular structure determined by X-ray diffraction [14] revealed an axially bonded unidentate catecholato ligand, which is formed via free-radical coupling between the cobaloxime(II) and the semiquinone anion radical ($DBSQ^-$•). The latter has been detected by EPR spectroscopy during the reaction together with its cobaloxime(III)-bonded derivative $Co^{III}(DBSQ^-•)$, which indicates a free-radical mechanism for catechol oxidation. The mechanism proposed for the catalytic oxidation on the basis of the detectable intermediates is shown in Fig. 7. In this scheme $Co^{II}$ stands for $[Co^{II}(Hdmg)_2(PPh_3)]$. The double catalytic cycle is joined together by $Co^{II}$, and $O_2$-activation takes place via formation of superoxocobaloxime(III), $Co^{III}O_2$, followed by H-atom abstraction from $DBCatH_2$, affording $DBSQ^-$•. During the catalytic reaction, $O_2$-uptake and catechol oxidation are taking place according to the lower cycle, while the cobaloxime species in the upper cycle are present at steady state or equilibrium concentrations.

A detailed kinetic study [16] of the cobaloxime(II) catalyzed oxidation of $DBCatH_2$ has confirmed the validity of general kinetic equation (1). It corresponds to a situa-

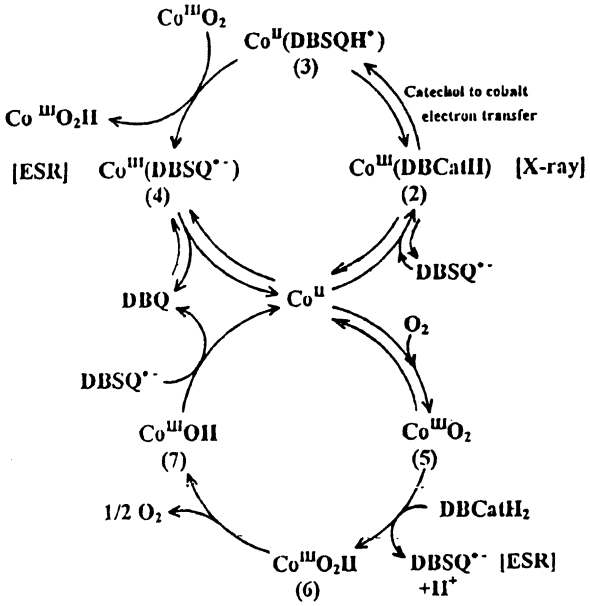


Fig. 7. Double catalytic cycle of the oxidation of $DBCatH_2$.

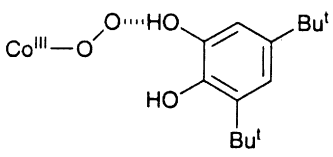


X

Fig. 8. Proposed structure of intermediate X.

tion when none of the species concentrations involved in pre-equilibria $K_1$ and $K_2$ are negligible, therefore, all species should be included into the mass balance equations for the given system.

For the $DBCatH_2$ system, self-consistent kinetic results are obtained on the assumption that $1 \ll K_2[DBCatH_2]_o$, which simplifies general equation (1) to equation (4). The parameters obtained from the latter are listed in Table 1.

$$v_{in} = k_3 \frac{K_1 K_2 [O_2][DBCatH_2]_o[Co]_o}{1 + K_1 K_2 [O_2][DBCatH_2]_o} \quad (4)$$

The observed kinetic behavior is consistent with the reaction mechanism (5)–(13).

$$Co^{II} + O_2 \rightleftarrows Co^{III}O_2 \quad K_1 \quad (5)$$

$$Co^{III}O_2 + DBCatH_2 \rightleftarrows X \quad K_2 \quad (6)$$

$$X \rightleftarrows Co^{III}O_2H + DBSQ^{\bullet -} + H^+ \quad k_3 \quad (7)$$

$$Co^{II} + DBSQ^{\bullet -} \rightleftarrows Co^{III}(DBCatH) \quad (8)$$

$$2Co^{II} + O_2 + DBCatH_2 \rightarrow Co^{III}(DBCatH) + Co^{III}O_2H \quad (9)$$

$$2Co^{III}O_2H \rightarrow 2Co^{III}OH + O_2 \quad (10)$$

$$Co^{III}OH + DBSQ^{\bullet -} + H^+ \rightarrow Co^{II} + DTBQ + H_2O \quad (11)$$

$$Co^{III}OH + Co^{III}(3,5\text{-}DBCatH) \rightarrow Co^{II} + Co^{III}(DBSQ^{\bullet -}) + H_2O \quad (12)$$

$$Co^{III}(DBSQ^{\bullet -}) \rightleftarrows Co^{II} + DTBQ \quad (13)$$

The kinetic behavior requires the formation of intermediate X (Fig. 8), which decomposes in the rate-determining H-atom abstraction step. In the steady state following the fast initial phase the overall stoichiometry requires that $O_2$ be reduced to $H_2O$, rather than $H_2O_2$, therefore, the hydroperoxocobaloxime $Co^{III}O_2H$ formed in step (7) should undergo disproportionation, regenerating one half of the $O_2$ absorbed and producing the hydroxocobaloxime $Co^{III}OH$ (step 10). Also, for a sustained catalytic cycle to occur in the steady state, a route to the product DTBQ and a path regenerating the $Co^{II}$ catalyst are necessary. These requirements of a catalytic cycle are fulfilled by addition of electron transfer steps (11) and (12) to the mechanism. Formation of the cobaloxime derivative $Co^{III}(DBSQ^{-}\bullet)$ exhibiting the eight-line ESR signal observed during the catalytic oxidation can be explained by reaction (12). It is also involved in equilibrium (13), which has been demonstrated by reacting cobaloxime(II) with DTBQ under $N_2$, when the same ESR spectrum was obtained.

A remarkable feature of mechanism (5)–(13) is that the dioxygen activation steps (5) and (6) are involved in both the rapid initial phase and the steady state. They control the rate of dioxygen uptake by the reacting solution, which, however, differs very strongly in these two phases. This implies that as the system reaches the steady state very shortly after mixing the reactants, the concentration of $Co^{II}$ drops to a fraction of the starting value, so that the $O_2$ consumption rate falls from the stopped-flow level [9] to values susceptible to monitoring by gas volumetry.

### 2.6. Oxygenative cleavage of the stilbene double bond

In the presence of the cobaloxime(II) catalyst [Co(Hdmg)$_2$(Ph$_3$P)$_2$], at room temperature and 1 atm $O_2$ or air, 3,3′,5,5′-tetra-*tert*-butyl-4,4′-dihydroxystilbene ($H_2$StQ) undergoes oxidative dehydrogenation to the corresponding stilbenequinone (StQ), and parallel oxidative cleavage with double oxygen insertion at the C=C bond to afford 2,6-di-*tert*-butyl-4-hydroxybenzaldehyde (Ald, Fig. 9) [17]. The relative contribution of these two stoichiometries depends on the degree of $H_2$StQ conversion.

In the steady state, the relative rate of formation of StQ and Ald is approximately constant throughout a given run, indicating that they are formed in competitive reactions, via a common free-radical intermediate StQ$^{-}\bullet$ (Fig. 10) detected by EPR spectroscopy during the reaction.

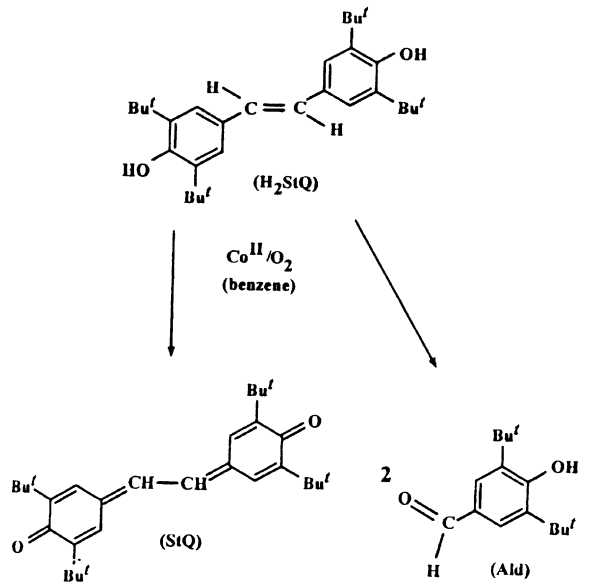


Fig. 9. Cleavage of stilbene derivative $H_2$StQ with double O-insertion.

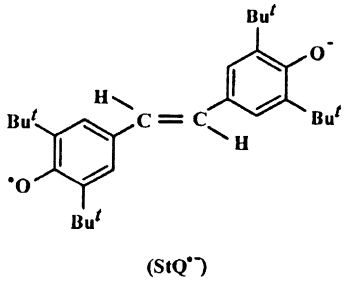


Fig. 10. Free-radical intermediate derived from $H_2StQ$.

The kinetics of the catalytic oxidation has been studied by a volumetric technique at constant pressure. The observed kinetic behavior is consistent with the reaction mechanism (14)–(20), where $Co^{II}$ and $Co^{III}$ represent the $[Co^{II}(Hdmg)_2(Ph_3P)]$ and $[Co^{III}(Hdmg)_2(Ph_3P)]^+$ moiety, respectively.

$$Co^{II} + O_2 \rightleftarrows Co^{III}O_2 \quad K_1 \tag{14}$$

$$Co^{III}O_2 + H_2StQ \rightleftarrows X \quad K_2 \tag{15}$$

$$X \rightarrow Co^{III}O_2H + StQ^{\bullet-} \quad k_3 \tag{16}$$

$$2Co^{III}O_2H \rightarrow 2Co^{III}OH + O_2 \quad \text{fast} \tag{17}$$

$$Co^{III}OH + StQ^{\bullet-} \rightarrow Co^{II} + StQ + H_2O \quad \text{fast} \tag{18}$$

$$Co^{III}O_2 + StQ^{\bullet-} \rightarrow CoOOR^- \quad \text{fast} \tag{19}$$

$$CoOOR^- \rightarrow 2Ald + Co^{II} \quad \text{fast} \tag{20}$$

The rate law corresponding to the proposed mechanism can be derived by assuming that steps (14) and (15) are reversible and step (16) is rate-determining. Disproportionation (17) can be regarded as fast [9], consequently, the concentration of $Co^{III}O_2H$ is negligible. As the kinetics were determined from initial rates and the formation of Ald is delayed relative to that of StQ, steps (19) and (20) can be disregarded and the concentration of $CoOOR^-$ is also negligible. These considerations lead to rate equation (21), which is identical in form with the general equation (1), i.e., consistent with the kinetic behavior without simplifying assumptions.

$$v_o = k_3[Co]_o \frac{K_1K_2[O_2][H_2StQ]}{1 + K_1[O_2]\{1 + K_2[H_2StQ]\}} \tag{21}$$

Formation of the aldehyde product requires a reaction between $Co^{III}O_2$ and $StQ^-\bullet$ in which the latter is attacked in its mesomeric form with the unpaired electron at one of the olefinic carbon atoms. The alkylperoxocobaloxime(III) formed will decompose to the aldehyde probably via a dioxetane intermediate. The required protons are derived from the water present in ordinary benzene. The proposed reaction mechanism is depicted in Fig. 11.

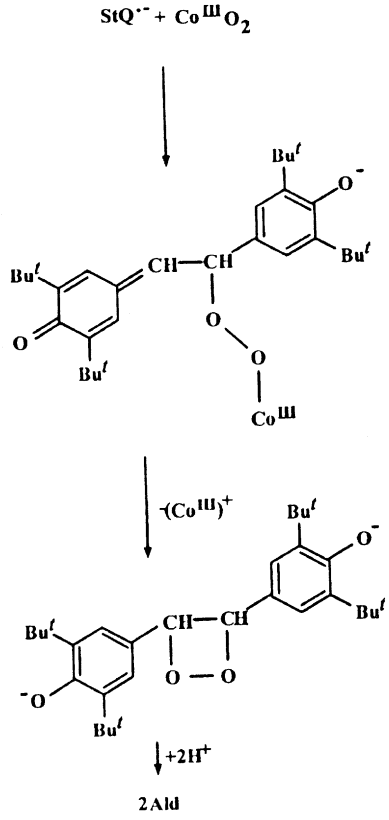


Fig. 11. Aldehyde formation from $StQ^-\bullet$ via a dioxetane intermediate.

### 2.7. Oxygen insertions catalyzed by cobaloxime(II)

Cobaloxime(II) catalyzes formal O-atom insertion into triphenylphosphine, alkyl isocyanides and nitrosobenzene [6,7].

Similarly, O-atom insertion was also observed in the case of benzimidazole, which was converted to bis(*N*-oxide) in the presence of cobaloxime(II) (cf. Fig. 2) [11].

Double oxygen insertion takes place in the oxidative bond cleavage of 3,3′,5,5′-tetra-*tert*-butyl-4,4′-dihydroxystilbene (cf. Fig. 11): the olefinic bond is split, affording two substituted benzaldehydes.

## 3. Ferroxime(II)-catalyzed oxidation of $DBCatH_2$ by $O_2$

After solvolysis $[Fe(Hdmg)_2(MeIm)_2]$ activates dioxygen in MeOH solution at room temperature and catalyses the oxidative dehydrogenation of $DBCatH_2$ to the corresponding DTBQ [4,19].

The kinetics of catalytic oxidation was followed by recording the dioxygen absorption curves as a function of time. From these curves the initial rates ($V_{in}$) of dioxygen uptake were determined as a function of catalyst and substrate concentration as well as dioxygen partial pressure.

The observed kinetics is consistent with mechanism (22)–(28) (N = MeIm), from which the kinetic equation (29) can be derived [4]. The assumption that $1 \ll K_2\,[\mathrm{DBCatH_2}]_o$ converts the general equation (1) to the form (29).

$$[\mathrm{Fe^{II}N_2}] + \mathrm{MeOH} \overset{K_s}{\rightleftarrows} [\mathrm{Fe^{II}N(MeOH)}] + \mathrm{N} \quad \text{(solvolysis)} \tag{22}$$

$$[\mathrm{Fe^{II}N}] + \mathrm{O_2} \overset{K_1}{\rightleftarrows} [\mathrm{Fe^{III}N}(\mathrm{O_2^-})] \quad \text{(pre-equilibrium)} \tag{23}$$

$$[\mathrm{Fe^{III}N}(\mathrm{O_2^-})] + \mathrm{DBCatH_2} \overset{K_2}{\rightleftarrows} [(\mathrm{Fe^{III}N}(\mathrm{O_2^-}) \cdots \mathrm{H_2DBCat})] \quad \text{(pre-equilibrium)} \tag{24}$$

$$[(\mathrm{Fe^{III}N}(\mathrm{O_2^-}) \cdots \mathrm{H_2DBCat})] \overset{k_3}{\rightleftarrows} [\mathrm{Fe^{III}N(O_2H)}] + \mathrm{DBSQ^{\bullet -}} + \mathrm{H^+} \quad \text{(slow)} \tag{25}$$

$$[\mathrm{Fe^{II}N}] + \mathrm{DBSQ^{\bullet -}} \overset{K_4}{\rightleftarrows} [\mathrm{Fe^{II}N(DBSQ^{\bullet -})}]^-_{\text{(blue)}} \quad \text{(equilibrium)} \tag{26}$$

$$[\mathrm{Fe^{III}N(O_2H)}] + \mathrm{DBSQ^{\bullet -}} + \mathrm{H^+} \overset{k_5}{\rightarrow} [\mathrm{NFe^{IV}O}] + \mathrm{DTBQ} + \mathrm{H_2O} \tag{27}$$

$$[\mathrm{NFe^{IV}O}] + \mathrm{H_2DBCat} \overset{k_6}{\rightarrow} [\mathrm{Fe^{II}N}] + \mathrm{DTBQ} + \mathrm{H_2O} \quad \text{(fast)} \tag{28}$$

In the catalytic process steps (23) and (24) can be regarded as pre-equilibria and (25) as the rate-determining step. Reversibility is often encountered in dioxygen coordination to iron(II), which is in support of step (23). Hydrogen bonding of the substrate to the superoxo ligand is similar to that observed in the case of the analogous superoxocobaloxime(III). In step (27) an electron from $\mathrm{DBSQ^-}\bullet$ is utilized for the proton-assisted reductive heterolytic splitting of the O–O bond, producing a reactive ferryl species. The latter rapidly oxidises a second $\mathrm{DBCatH_2}$ molecule in step (28).

$$V_{\text{in}} = \frac{k_3 K_1 K_2 [\mathrm{O_2}][\mathrm{DBCatH_2}]_o [\mathrm{Fe}]_o}{1 + K_1 K_2 [\mathrm{O_2}][\mathrm{DBCatH_2}]_o} \tag{29}$$

## 4. Kinetic results

The kinetics and mechanisms of the oxidations catalyzed by cobaloxime(II) and ferroxime(II) are very similar. The kinetic results obtained for the systems studied are collected in Table 1. The observed rate constant is governed by the product given in the last column. The reactivity order (relative rate) for cobaloxime(II) is $\mathrm{DBCatH_2}$ (30.0) > AP (16.8) > $\mathrm{H_2StQ}$ (1.0). The cobaloxime-catalyzed oxidation of $\mathrm{DBCatH_2}$ is 3.6 times faster than the ferroxime-catalyzed reaction.

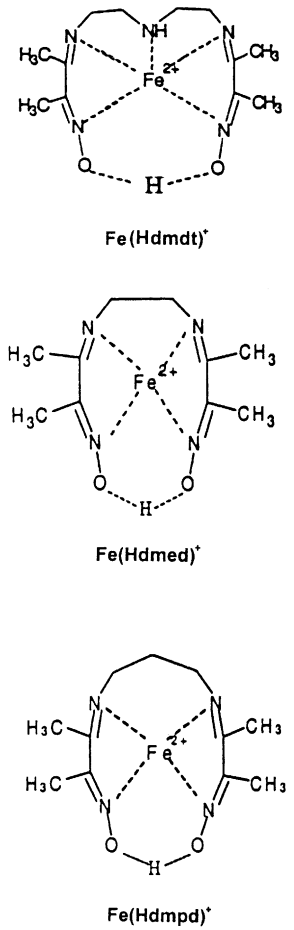


Fig. 12. New hydroxyimino Schiff-base complexes of iron(II) used as catalysts in $\mathrm{DBCatH_2}$ oxidation.

## 5. Oxidation of $\mathrm{DBCatH_2}$ catalyzed by hydroxyimino Schiff-base complexes of iron(II)

In order to explore the role of catalyst structure on its activity in catechol oxidation, we have synthesised the dioximatoiron(II) complexes shown in Fig. 12. The synthetic method involves the reaction of ethylenediamine (en), 1,3-propylenediamine (pd) and diethylenetriamine (dt) with diacetyl monoxime (dm) in methanol to form quadridentate and quinquedentate Schiff-base ligands. The resulting ligands (denoted as $\mathrm{H_2}$dmed, $\mathrm{H_2}$dmpd and $\mathrm{H_2}$dmdt) were reacted with iron(II) formate to obtain the new complexes. $\mathrm{Fe(Hdmed)^+}$, $\mathrm{Fe(Hdmpd)^+}$ and $\mathrm{Fe(Hdmdt)^+}$ have been identified by elemental analysis, spectrophotometric titration and electrospray mass spectroscopy (Table 2) [18,20]. Attempts to obtain X-ray quality crystals were unsuccessful.

As opposed to the stable, H-bonded, square-planar structure of the cobaloxime(II) and ferroxime(II) complexes, the dioximato species in Fig. 12 have more flexible ligand environments, which is expected to influence their catalytic (catecholase) activity.

Table 2
ES–MS peaks of the new hydroxyimino Schiff-base complexes

| Complex | *m/z* |
|---|---|
| $[Fe^{III}(Hdmed)]^+$ | 281.11 |
| $[Fe^{III}(Hdmpd)]^+$ | 295.14 |
| $[Fe^{III}(Hdmdt)]^+$ | 324.19 |

The complexes in Table 2 exhibit catecholase activity at room temperature, which was monitored in MeOH by the oxidation of $DBCatH_2$ as substrate. According to gas-volumetric measurements, $O_2$ absorption is only observed if both catalyst and substrate are present in the solution. Formation of a 1:1 mixed-ligand complex between catalyst and substrate has been detected by UV–vis spectrophotometry under $N_2$ for all of the three iron complexes. The latter show no reactivity or spectral changes when exposed to $O_2$ alone. However, dioxygen uptake starts as soon as $DBCatH_2$ is added. An iron-bound semiquinone anion radical has been detected by ESR spectroscopy, indicating the stepwise nature of catechol oxidation.

In order to obtain a quantitative measure of the catecholase activity, we have carried our detailed kinetic studies of the oxidation of $DBCatH_2$ by measuring the initial rates of dioxygen uptake by the reacting solution. The kinetic behavior is consistent with the reaction mechanism (30)–(34), which leads to kinetic equation (35). The kinetic and equilibrium parameters obtained from the latter are listed in Table 3.

Pre-equilibria:

$$[Fe^{II}(HL)]^+ + DBCatH_2 \overset{K_1}{\rightleftarrows} [(HL)Fe^{II}(DBCatH)] + H^+ \quad (30)$$

$$[(HL)Fe^{II}(DBCatH)] + O_2 \overset{K_2}{\rightleftarrows} [(H_2L)Fe^{III}(DBCatH)O_2] \quad (31)$$

Rate-determining step (H-atom or $e^-/H^+$ transfer):

$$[(HL)Fe^{III}(DBCatH)O_2] \overset{k_3}{\rightleftarrows} \underset{\text{Fe-bound semiquinone anion radical (ESR)}}{[(HL)Fe^{III}(DBSQ^{\bullet -})(O_2H)]} \quad (32)$$

Homolytic O–O bond cleavage:

$$[(HL)Fe^{III}(DBSQ^{\bullet -})(O_2H)] \overset{\text{fast}}{\rightarrow} DTBQ + [(HL)Fe^{IV}O]^+ + OH^- \quad (33)$$

$$[(HL)Fe^{IV}O]^+ + DBCatH_2 \overset{\text{fast}}{\rightarrow} [Fe^{II}(HL)]^+ + DTBQ + H_2O \quad (34)$$

where $H_2L = H_2$dmed, $H_2$dmpd, $H_2$dmdt; $DBSQ^{-}\bullet$ = semiquinone anion radical; DTBQ = 3,5-di-*tert*-butyl-*o*-quinone.

The above mechanism takes account of the fact that $[Fe^{II}(HL)]^+$ does not react with $O_2$, therefore, a catecholato mixed-ligand complex should form before any $O_2$ uptake. The kinetic behavior associated with two equilibria followed by the rate-determining step corresponds to general equation (1), as also observed in the case of cobaloxime(II) and ferroxime(II) catalyzed oxidations. As the rate shows no saturation type behavior with increasing $O_2$ pressure in the interval used, we conclude that $1 \gg K_2[O_2]$, which leads to a simplified equation (35). It affords $K_1$ and $k_3K_2$ as well as the apparent rate constant $k_3K_1K_2$ (Table 3). The trends emerging from the data indicate the importance of steric factors: the stability of the mixed-ligand complex $K_1$ is the highest for $[Fe(Hdmed)]^+$ presenting the weakest steric hindrance against catechol coordination, affording the largest rate of oxidation ($k_3K_1K_2$).

$$V_{in} = \frac{k_3K_1K_2[O_2][H_2DBCat]_o[Fe]_o}{1 + K_1[DBCatH_2]_o} \quad (35)$$

In the presence of $[Fe(dmdt)]^+$ and an excess of triethylamine, in addition to the *o*-quinone, formation of the intradiol cleavage product of $DBCatH_2$ is also observed. This is in line with our expectations based on the flexibility of the ligand environment of the iron center in $[Fe(dmdt)]^+$. Apparently, bidentate catechol coordination becomes feasible, which opens up a new reaction path favouring oxygenative cleavage. A kinetic study to obtain mechanistic information on the dioxygenation route is in progress.

Table 3
Rate and equilibrium constants determined using kinetic equation (35)

| Catalyst | $K_1$ ($M^{-1}$) | $k_3K_2$ ($M^{-1}\,s^{-1}$) |
|---|---|---|
| $[Fe(Hdmed)]^+$ no TEA | 64.7 ± 3.5 | 4.5 ± 0.2 |
| $[Fe(Hdmpd)]^+$ no TEA | 11.1 ± 0.5 | 5.5 ± 0.3 |
| $[Fe(Hdmpd)]^+$ TEA added | 317 ± 0.5 | 14.2 ± 0.3 |
| $[Fe(Hdmdt)]^+$ no TEA | 6.5 ± 0.3 | 8.7 ± 0.4 |

## 6. Conclusion and trends

Investigations on the kinetics and mechanism of the catecholase reaction catalyzed by oximatocobalt(II) and oximatoiron(II) complexes have shown the validity of the general kinetic equation (4), consistent with a mechanism involving ternary complex formation between catalyst, substrate and dioxygen. The rate-determining step is H-atom transfer to a superoxo ligand within this complex, affording an intermediate semiquinone anion radical. In one remarkable case, a free-radical mechanism was found to operate in the oxidative cleavage of the stilbene double bond. New oximatoiron(II) complexes of hydroxyimino Schiff bases have been synthesized and their catecholase activities demonstrated. Work is in progress to structurally characterize the new catalyst complexes and to examine similar complexes with other metals.

The chemistry of non-heme type catecholase and catechol dioxygenase models poses a number of fundamental mechanistic problems, which attract widespread attention. One of the major features of the biomimetic systems is the di-

chotomy of products, viz. the formation of *o*-quinones and cleavage products with a varying degree of selectivity. Interpretation of this behavior requires special and detailed kinetic studies combined with identification of reactive intermediates, some of which may be quite elusive. A case in point is oxoiron(IV), whose formation has recently been elegantly demonstrated for some non-heme iron complexes subjected to treatment with single oxygen atom donors [1n]. The type of catechol binding to the catalyst complex is of great importance in governing the reactivity pattern. Both unidentate and bidentate coordination are possible, as is hydrogen bonding of a catechol OH group to a coordinated superoxo ligand (cf. Eq. (24)). A factor of utmost importance is the flexibility (mobility) of ligands in the coordination sphere, which is expected to influence catechol coordination. Structural studies of mixed-ligand complexes with catecholato ligands using X-ray diffraction (by single crystals and in solution), Mössbauer, Electron Spin Resonance and NMR spectroscopy, as well as electrospray mass spectroscopy are underway.

## Acknowledgements

This work was supported by the Hungarian Science Fund (OTKA Grant T 029036).

## References

[1] (a) L.I. Simándi, Catalytic Activation of Dioxygen by Metal Complexes, Kluwer Academic Publishers, Dordrecht, 1992 (Chapter 5);
(b) C.G Pierpont, C.W. Lange, in: K.D. Karlin (Ed.), Progress in Inorganic Chemistry, vol. 41, Wiley, New York, 1994, pp. 331–442;
(c) L. Que, in: J. Reedijk, E. Bouwman (Eds.), Bioinorganic Catalysis, Marcel Dekker, New York, 1999, pp. 269–321;
(d) T. Funabiki, in: T. Funabiki (Ed.), Oxygenases and Model Systems, Kluwer Academic Publishers, Dordrecht, 1997, pp. 19–104, 105–15;
(e) T. Funabiki, in: L.I. Simándi (Ed.), Advances in Catalytic Activation of Dioxygen by Metal Complexes, Kluwer Academic Publishers, Dordrecht, 2003, pp. 157–236 (Chapter 4);
(f) C. Xin Zhang, H.-C. Liang, K.J. Humphreys, K.D. Karlin, in: L.I. Simándi (Ed.), Advances in Catalytic Activation of Dioxygen by Metal Complexes, Kluwer Academic Publishers, Dordrecht, 2003, pp. 79–121 (Chapter 2);
(g) L.I. Simándi, in: L.I. Simándi (Ed.), Advances in Catalytic Activation of Dioxygen by Metal Complexes, Kluwer Academic Publishers, Dordrecht, 2003, pp. 265–328 (Chapter 6);
(h) A. Nishinaga, in: T. Funabiki (Ed.), Oxygenases and Model Systems, Kluwer Academic Publishers, Dordrecht, 1997, pp. 157–194;
(i) J. Wikaira, S.M. Gorun, in: J. Reedijk, E. Bouwman (Eds.), Bioinorganic Catalysis, Marcel Dekker, New York, 1999, pp. 355–422;
(j) L. Que, M.F. Reynolds, in: A. Sigel, H. Sigel (Eds.), Metal Ions in Biological Systems, vol. 37, Marcel Dekker, New York, 2000, pp. 505–525;
(k) T. Klabunde, C. Eicken, J. C. Sacchettini, B. Krebs, Nat. Struct. Biol. 5 (1998) 1084;
(l) P. Gentschev, N. Moller, B. Krebs, Inorg. Chim. Acta 300 (2000) 442;
(m) M. Merkel, F.K. Muller, B. Krebs, Inorg. Chim. Acta 337 (2002) 308;
(n) J.-U. Rohde, J.-H. In, M.H. Lim, W.W. Brenessel, M.R. Bukowski, A. Stubna, E. Münck, W. Nam, L. Que, Science 229 (2003) 1037.
[2] L.I. Simándi, T. Barna, Z. Szeverényi, S. Németh, Pure Appl. Chem. 64 (1992) 1511.
[3] L.I. Simándi, Int. Rev. Phys. Chem. 8 (1989) 21.
[4] T.L. Simándi, L.I. Simándi, J. Chem. Soc. Dalton Trans. (1999) 4529.
[5] L.I. Simándi, C.R. Savage, Z.A. Schelly, S. Németh, Inorg. Chem. 21 (1982) 2765.
[6] S. Németh, Z. Szeverényi, L.I. Simándi, Inorg. Chim. Acta Lett. 44 (1980) L107.
[7] S. Németh, L.I. Simándi, Inorg. Chim. Acta Lett. 64 (1982) L21.
[8] L.I. Simándi, A. Fülep-Poszmik, S. Németh, J. Mol. Catal. 48 (1988) 265.
[9] S. Németh, A. Fülep-Poszmik, L.I. Simándi, Acta Chim. Acad. Sci. Hung. 110 (1982) 461.
[10] S. Németh, L.I. Simándi, J. Mol. Catal. 14 (1982) 87.
[11] S. Németh, L.I. Simándi, J. Mol. Catal. 14 (1982) 241.
[12] L.I. Simándi, T.M. Barna, L. Korecz, A. Rockenbauer, Tetrahedron Lett. 34 (1993) 717.
[13] L.I. Simándi, T.M. Barna, S. Németh, J. Chem. Soc. Dalton Trans. (1996) 473.
[14] L.I. Simándi, T.M. Barna, Gy. Argay, T.L. Simándi, Inorg. Chem. 34 (1995) 6337.
[15] T.L. Simándi, L.I. Simándi, React. Kinet. Catal. Lett. 65 (1998) 301.
[16] L.I. Simándi, T.L. Simándi, J. Chem. Soc. Dalton Trans. (1998) 3275.
[17] L.I. Simándi, T.L. Simándi, J. Mol. Catal. A 117 (1997) 299.
[18] L.I. Simándi, Z. May, G. Besenyei, A. Vértes, T. Funabiki, in: Proceedings of the 35th International Conference on Coordination Chemistry, Heidelberg, July 22–26, 2002, p. 86 (Abstracts O 3.10).
[19] L.I. Simándi, T.L. Simándi, J. Inorg. Biochem. 86 (2001) 432.
[20] Z. May, G. Besenyei, L.I. Simándi, D. Asari, T. Funabiki, J. Inorg. Biochem. 86 (2001) 332.